nature cell biology

Atrophy of *S6K1*$^{-/-}$ skeletal muscle cells reveals distinct mTOR effectors for cell cycle and size control

Mickaël Ohanna[1], Andrew K. Sobering[1], Thomas Lapointe[1], Lazaro Lorenzo[1], Christophe Praud[1], Emmanuel Petroulakis[2], Nahum Sonenberg[2], Paul A. Kelly[1], Athanassia Sotiropoulos[1,3] and Mario Pende[1,3]

The mammalian target of rapamycin (mTOR) and Akt proteins regulate various steps of muscle development and growth, but the physiological relevance and the downstream effectors are under investigation[1–6]. Here we show that S6 kinase 1 (S6K1), a protein kinase activated by nutrients and insulin-like growth factors (IGFs), is essential for the control of muscle cytoplasmic volume by Akt and mTOR. Deletion of S6K1 does not affect myoblast cell proliferation but reduces myoblast size to the same extent as that observed with mTOR inhibition by rapamycin. In the differentiated state, *S6K1*$^{-/-}$ myotubes have a normal number of nuclei but are smaller, and their hypertrophic response to IGF1, nutrients and membrane-targeted Akt is blunted. These growth defects reveal that mTOR requires distinct effectors for the control of muscle cell cycle and size, potentially opening new avenues of therapeutic intervention against neoplasia or muscle atrophy.

Adaptive changes in skeletal muscle mass are correlated with the activity of the mTOR pathway. Growth during resistance exercise, functional overload and high-protein diet is accompanied by the upregulation of mTOR, whereas inactivity, glucocorticoid therapy and food deprivation lead to mTOR inhibition and muscle atrophy[7]. The mTOR kinase resides in a protein complex that integrates two major anabolic inputs for muscle, the branched-chain amino acids and IGFs[8,9]. The function of mTOR in muscle has been inferred by employing rapamycin, an mTOR inhibitor[8]. Rapamycin attenuates IGF1-induced proliferation, survival, differentiation and hypertrophy in muscle cell lines, indicating that mTOR participates at different levels in the muscle developmental programme[1,4,10,11]. Less clear are the molecular targets of such regulatory events. Two families of mTOR substrates have been characterized: the ribosomal protein S6 kinases (S6K1–2), and the eIF4E-binding proteins (4EBP1–3)[8]. Both protein families interact with the translational machinery; the S6Ks phosphorylate the S6 protein of small ribosomal subunits (rpS6) and the 4EBPs bind to the mRNA cap-binding protein eIF4E. Although recent work in *Drosophila* and mammalian cells is consistent with a role of S6K and 4EBP in mediating TOR functions[12–16], the exact contribution of these signalling molecules awaits demonstration[13,17].

To determine whether S6K1 and/or S6K2 deletion reduces skeletal muscle mass, we compared the weight of gastrocnemius (GC) and tibialis anterior (TA) muscles from wild-type and double-mutant *S6K1*$^{-/-}$;*S6K2*$^{-/-}$ mice. *S6K*-deficient mice had a reduced muscle mass, which persisted after normalization to body weight (Table 1). The decreased cross-sectional area (CSA) of soleus muscles in *S6K1*$^{-/-}$;*S6K2*$^{-/-}$ mice was correlated with a 20% reduction in the CSA of the fibres (Fig. 1a; Supplementary Fig. S1a), whereas the total number of fibres did not differ (Fig. 1b). Fibre atrophy was caused by the single deletion of *S6K1* (Fig. 1a). Immunostaining with antibodies against type I and type II myosin heavy chain showed no difference in fibre type composition of soleus and TA muscles (Table 1, Fig. 1c; Supplementary Fig. S1b). However, the decrease in CSA was similar in both fibre types (Supplementary Fig. S1b).

Muscle atrophy could stem from an impairment of myoblast cell fusion into the fibre and/or a decrease in the cytoplasmic domain regulated by one myonucleus. We evaluated cell fusion by counting the number of nuclei inside the sarcolemma and showed that the number of myonuclei per transverse fibre section was similar in the four genotypes (Fig. 1d). Taken together, these data show that fibre development, type specification and cell fusion are not altered in S6K-deficient mice. Thus, the reduced CSA of *S6K1*$^{-/-}$;*S6K2*$^{-/-}$ fibres is due to impaired growth of muscle syncytia. Strikingly, the deletion of *S6K1* is sufficient to reproduce this atrophic phenotype.

The reduction of muscle mass in S6K-deficient mice is accompanied by decreased body weight (Table 1; ref. 16) and the circulating insulin level is lower[18]. To exclude the possibility of systemic tissue size control in *S6K1*$^{-/-}$;*S6K2*$^{-/-}$ mice, we established primary cultures from wild-type and *S6K1*$^{-/-}$;*S6K2*$^{-/-}$ muscles. Both myoblast types expanded at similar rates in rich medium (Fig. 2a). To assess cell proliferation, asynchronously growing cells were incubated with bromodeoxyuridine (BrdU). Proliferation rate was not affected by *S6K* deletion, and rapamycin decreased the proliferation of both cultures equally (Fig. 2a, b), showing that control of the muscle cell cycle by mTOR requires neither S6K1 nor S6K2.

[1]Inserm, Avenir, U584, Université Paris 5, Faculté de Médecine Necker-Enfants Malades, 156 rue de Vaugirard, Paris, F-75730, France. [2]Department of Biochemistry and McGill Cancer Center, McGill University, McIntyre Medical Building, Montreal, Quebec, Canada H3G 1Y6.
[3]Correspondence should be addressed to M.P. (e-mail:pende@necker.fr) or A.S. (e-mail:sotiropoulos@necker.fr).

Published online: 20 February 2005; DOI: 10.1038/ncb1231

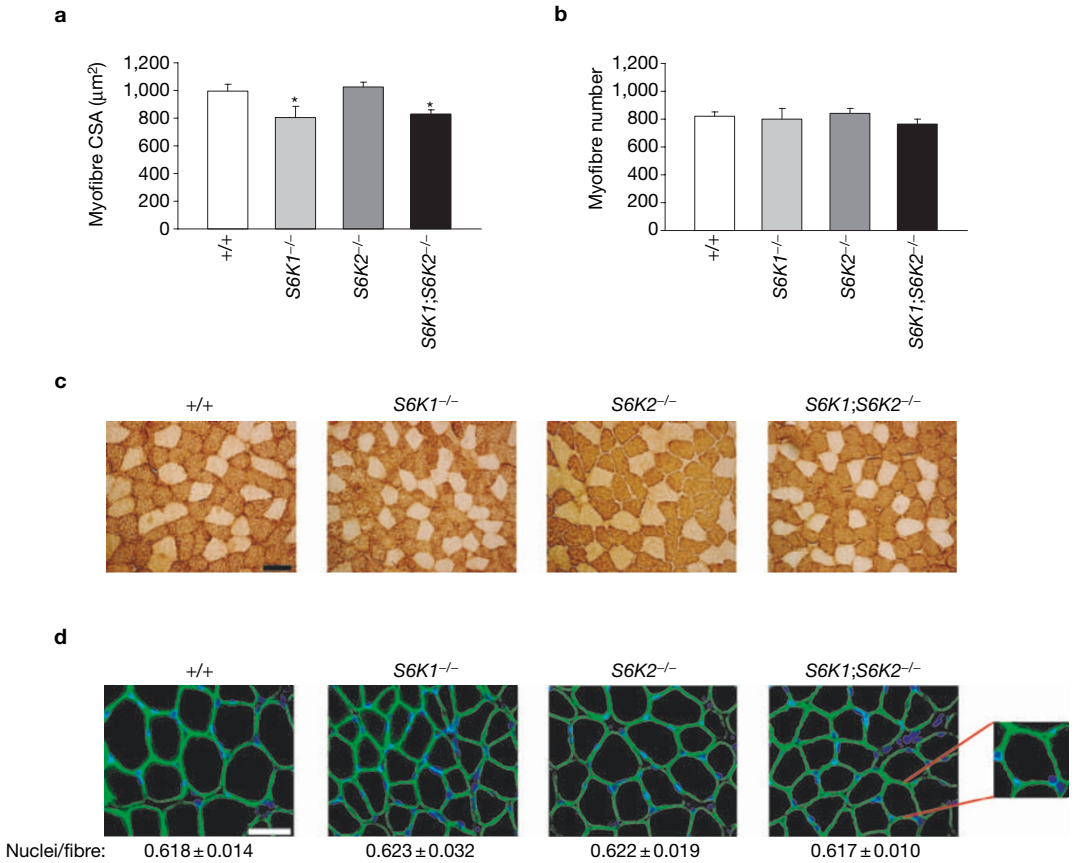

Figure 1 Atrophy of S6K1$^{-/-}$ muscles. (**a**,**b**) The CSA of individual soleus myofibres is reduced as a consequence of S6K1 deletion (**a**), whereas the myofibre number remains constant (**b**). All fibres in one section were analysed. Data are means±s.e.m. for at least four mice per genotype. (**c**) Fibre type is not affected by S6K deletion. Representative sections of soleus muscle immunostained with antibodies against type II MyHC are shown. The average percentage of myofibre types is indicated in Table 1. Scale bar, 50μm. (**d**) Number of myonuclei per fibre section is not affected by S6K deletion. Sections of soleus muscle were immunostained with anti-dystrophin antibodies and Hoechst 33258 to reveal sarcolemma and nuclei. The right panel is a higher-magnification image to show the distinction between nuclei inside (arrow) and outside (arrowhead)the sarcolemma. The number of myonuclei per transverse fibre section is indicated at the bottom of each panel. Data are means±s.e.m. for at least four mice per genotype, 200 fibres each. Scale bar, 50μm.

Because the overexpression of *S6K1* and *4EBP1* mutant alleles might change proliferation rates[16], we evaluated their contribution in myoblasts. We first overexpressed wild-type (WT-S6K1) and rapamycin-resistant (RR-S6K1) alleles of S6K1 by adenoviral transduction. Both kinase isoforms failed to stimulate cell proliferation of wild-type and mutant cells (Fig. 2b) but rescued rpS6 phosphorylation in *S6K1*$^{-/-}$;*S6K2*$^{-/-}$ cells (Fig. 2c). However, in the presence of rapamycin, RR-S6K1 expression conferred partial protection against the inhibitory effect of the drug on proliferation and rpS6 phosphorylation (Fig. 2b, c). Thus, the deletion of *S6K* genes is not sufficient to mimic the effects of rapamycin on proliferation, whereas expression of RR-S6K1 in part counteracts the effects of rapamycin. This paradox can be explained by three distinct models. First, RR-S6K1 might mediate an event that is not regulated by the wild-type kinase. Alternatively, S6K1 might promote cell cycle progression exclusively when the other mTOR effectors are inactive. Finally, S6K1 might participate in the physiological

Table 1 Muscle/body weight and fibre composition of wild-type and S6K-deficient mice

Variable	Wild type	*S6K1;2*$^{-/-}$	*S6K1*$^{-/-}$	*S6K2*$^{-/-}$
Body weight (g)	20.4±0.4	15.6±0.1**	15.3±0.8**	19.8±0.9**
GC weight (mg)	94.9±7.3	58.1±3.8**	n.d.	n.d.
GC/body weight (mgg^{-1})	4.6±0.3	3.7±0.2*	n.d.	n.d.
TA weight (mg)	29.7±1.9	19.8±1.2**	n.d.	n.d.
TA/body weight (mgg^{-1})	1.4±0.1	1.2±0.1	n.d.	n.d.
Soleus type I (%)	44.3±2.6	46.1±1.5	47.8±2.8	42.3±1.3
Soleus type II (%)	68.9±1.3	71.1±0.5	72.5±2.5	71.6±1.0

Values are for five-week-old male mice of the indicated genotypes. Data are means ±s.e.m. for at least six mice. n.d, not determined.
*P<0.05 versus wild type; **P<0.01 versus wild type.

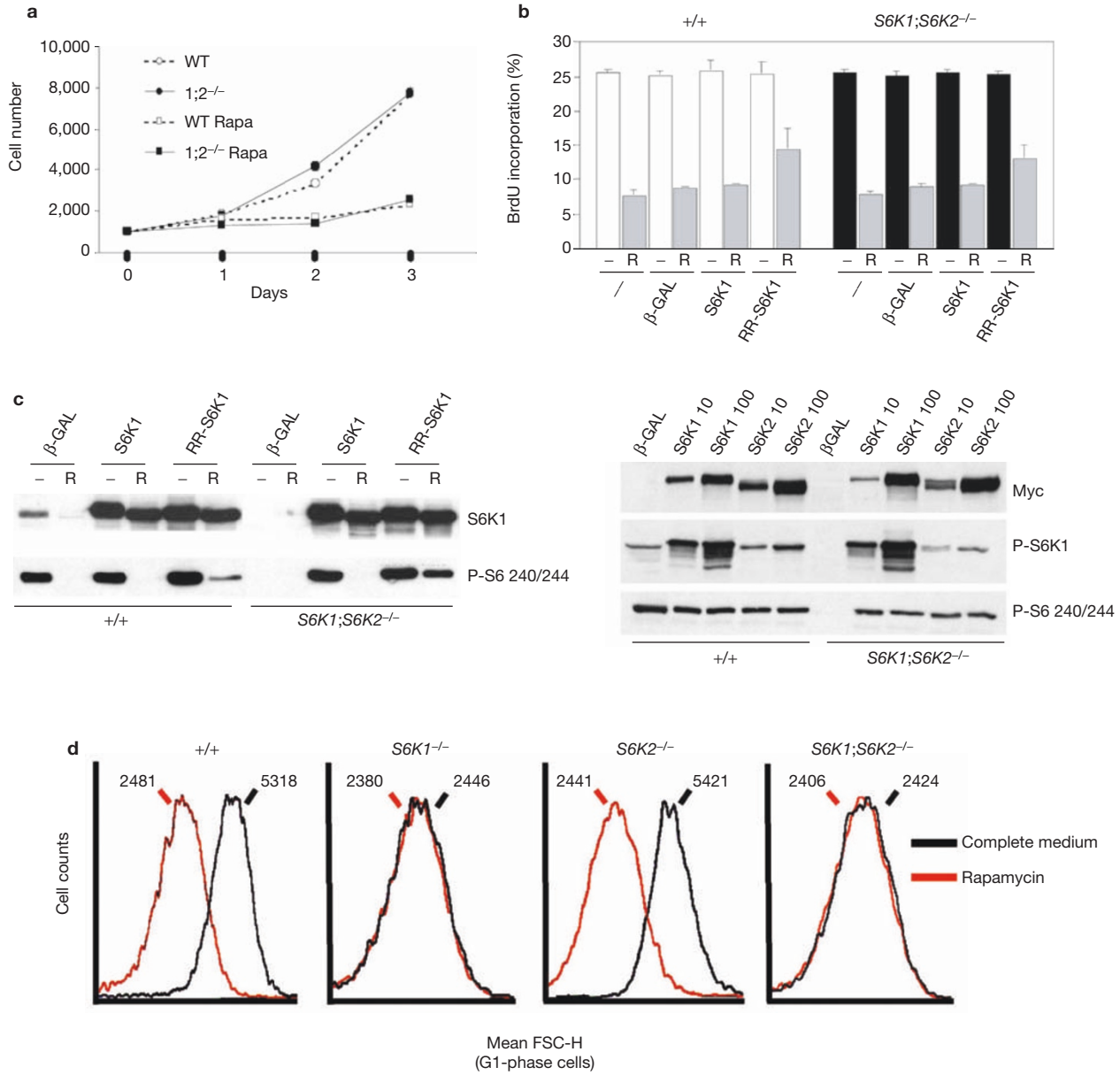

Figure 2 Myoblast proliferation and size show differential requirement for S6K1 activity. (**a**) Wild-type (WT; open symbols) and *S6K1*$^{-/-}$;*S6K2*$^{-/-}$ (filled symbols) cell doubling times are similar and equally sensitive to rapamycin. Myoblasts were grown in complete medium with (squares) or without (circles) 20 nM rapamycin (Rapa) and were counted on the indicated day. Data are means±s.e.m. for triplicate plates. The experiment was repeated three times with similar results. (**b**) Rapamycin inhibits S-phase entry of both wild-type and *S6K1*$^{-/-}$;*S6K2*$^{-/-}$ cells. Myoblasts were transduced with the indicated adenoviruses at a multiplicity of infection (MOI) of 100, grown for 2 days in the presence or absence of 20 nM rapamycin, and incubated for 1 h with BrdU. Cells were stained with anti-BrdU antibodies and Hoechst 33258 to reveal S-phase and total nuclei, respectively. Data are means±s.e.m. for the percentage of BrdU-positive cells (n=2). (**c**) Activities of different forms of S6 kinases. Immunoblot analysis of protein extracts from wild-type and *S6K1*$^{-/-}$;*S6K2*$^{-/-}$ myotubes using anti-Myc (to reveal Myc-tagged S6K), anti-phospho-S6K1 Thr389 and anti-phospho-rpS6 Ser240/244. Cells were transduced with the indicated S6K alleles at the myotube stage and harvested 2 days later for protein extraction. A dose of 100 MOI was used, unless otherwise indicated. Rapamycin treatment was during the last day of culture. (**d**) Cell size of S6K1 deficient cells is decreased and resistant to rapamycin. Forward scatter height (FSC-H) distribution of myoblasts during the G1 phase of the cell cycle is shown. The mean cell volume (μm^3) for each distribution is indicated. Cells were cultured for 3 days in complete medium in the presence (red line) or absence (black line) of 20 nM rapamycin. The experiments were repeated at least twice on five independent cultures with similar results.

control of the cell cycle, although this function is compensated for by other mTOR effectors when S6K is inactive.

To test whether 4EBP1 might represent the mTOR target controlling myoblast proliferation, we established cell lines expressing wild-type protein (4EBP1-WT) or a hypophosphorylated mutant (4EBP1-A) that constitutively binds to and inhibits eIF4E independently of mTOR activity[19]. Proliferation rates were not affected by the expression of 4EBP1-WT and 4EBP1-A (Supplementary Fig. S3a). Thus, the deletion of both S6K genes in combination with the expression of a hypophosphorylated 4EBP1 was not sufficient to mimic the effect of rapamycin on muscle cell proliferation, indicating that other mTOR effectors might be involved in this regulation.

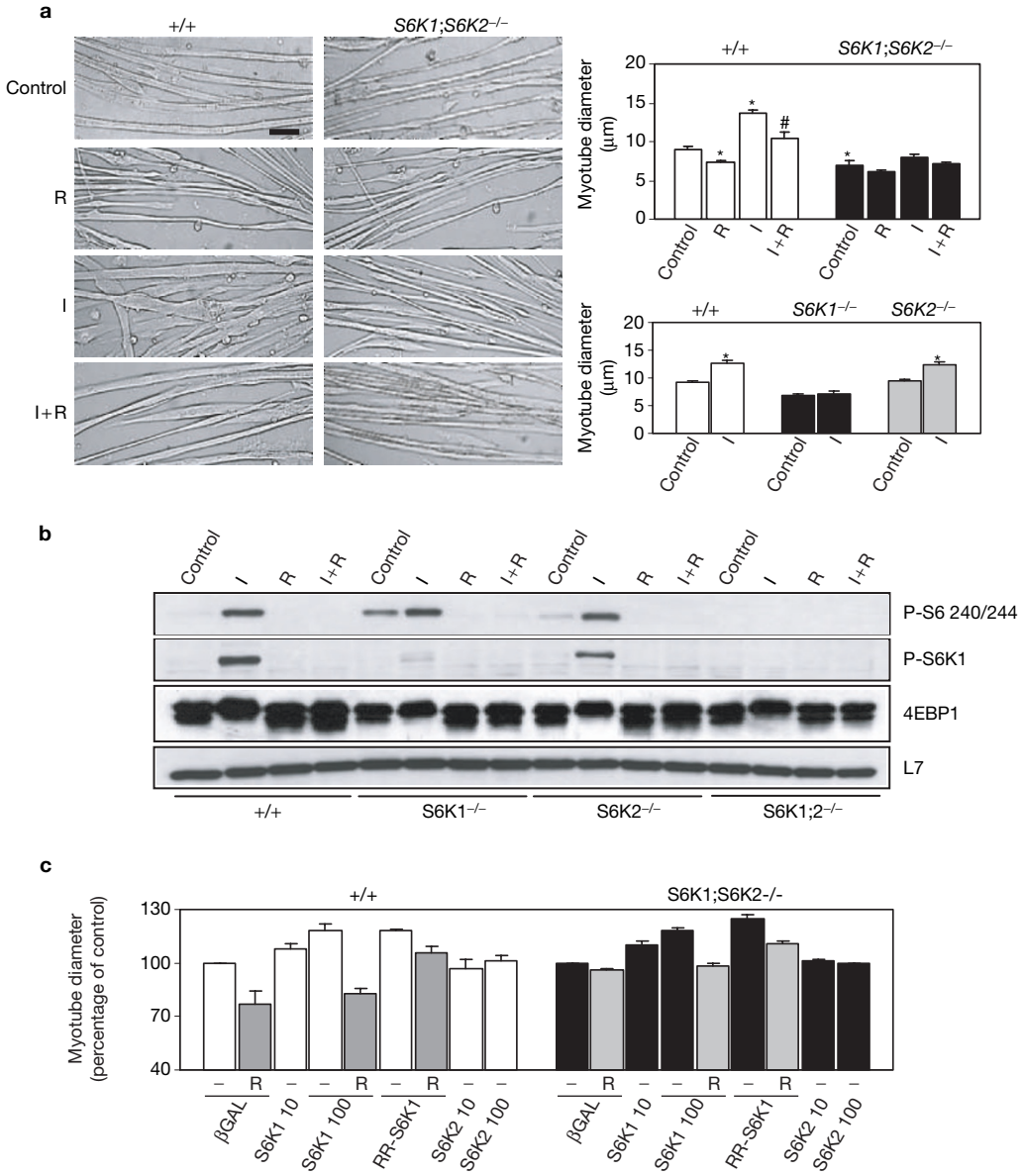

Figure 3 Normal myogenesis but impaired growth of S6K1$^{-/-}$ cells. (**a**) Effects of IGF1 (I) and rapamycin (R) on myotube hypertrophy are blunted in cells lacking S6K1. Bright-field images of myotube cell cultures from wild-type and *S6K1*$^{-/-}$;*S6K2*$^{-/-}$ mice are shown. Cells were allowed to differentiate for 2 days in 2% horse serum and then incubated for a further 2 days in the presence or absence of 20 nM rapamycin and 250 ng ml^{-1} IGF1-R3 in a medium containing 0.2% BSA. Myotube diameter was measured at day 4 of differentiation. Histograms are means±s.e.m. for at least four assays. Independent cell cultures were obtained from at least two mice of the indicated genotype. *, $P<0.01$ versus untreated wild type; #, $P<0.01$ versus IGF1-treated wild type. Scale bar, 20 μm. At least 400 myotubes were analysed. (**b**) S6 kinase activity in myotubes. Shown is an immunoblot analysis of protein extracts from myotubes of the indicated genotype, using anti-phospho-S6K1 Thr389, anti-phospho-rpS6 Ser240/244, anti-4EBP1 and anti-rpL7a antibodies, the last as a loading control. (**c**) Effect of S6K overexpression on myotube size. Myotubes were transduced with S6K or βGAL adenoviruses at 100 MOI, unless otherwise indicated. After 2 days of culture in 2% horse serum, the myotube diameter was measured and expressed as percentage change over βGAL-transduced cells. Histograms are means±s.e.m. for at least three experiments on two independent cultures. The average diameter of βGAL-transduced wild-type cells was 9.1±0.76 μm, and that of mutant cells was 6.79±0.26 μm.

By light microscopy, *S6K1*$^{-/-}$;*S6K2*$^{-/-}$ myoblasts appeared smaller than control cells. To measure cell size, forward scatter height was assayed by flow cytometry in myoblasts during the G1, S or G2/M phase of the cell cycle. Cell cycle distributions were identical (Supplementary Fig. S2a) but we observed size reduction in cells lacking both S6K genes compared with control (Fig. 2d). This decrease was pronounced during G1, though it was also detectable in the other phases (not shown). The deletion of *S6K1* was sufficient to decrease cell size, whereas *S6K2*$^{-/-}$ myoblasts were comparable to those in the control. Importantly, rapamycin treatment of wild-type and *S6K2*$^{-/-}$ myoblasts reduced cell size to the same extent as *S6K1* deletion.

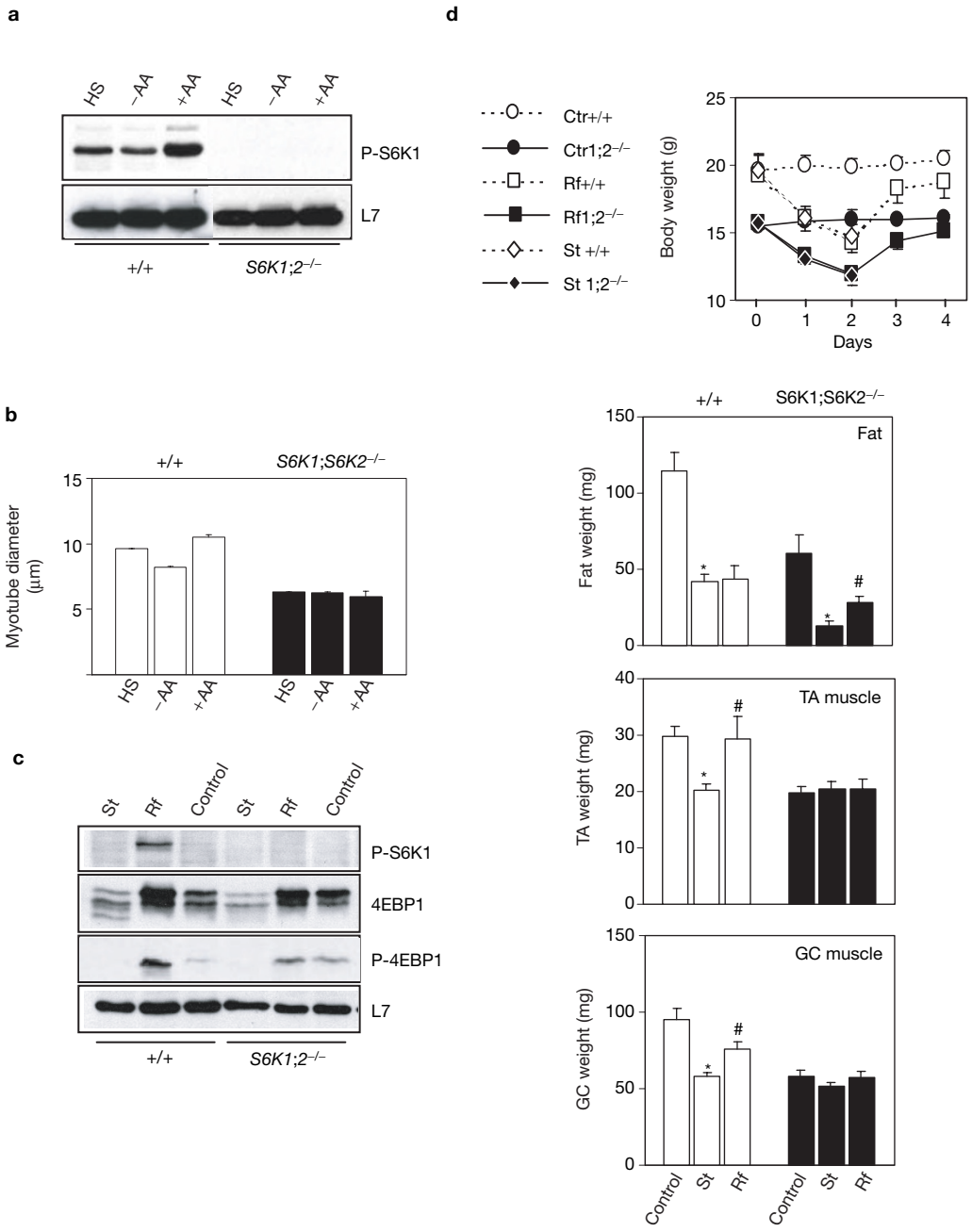

Figure 4 Nutritional cues requie S6K to affect muscle mass. (**a**) S6K activity in muscle cells is regulated by the levels of extracellular amino acids. Immunoblot analysis of protein extracts from myotubes of the indicated genotype, using anti-phospho-S6K1 Thr389 and anti-rpL7a antibodies, the latter as a loading control. Cells were allowed to differentiate for 3 days in 2% horse serum. Cells were then incubated for a further 2 days in amino-acid-free medium with (+AA) or without (–AA) addition of the complete amino acid set during the last hour before harvesting. Control cells were kept for 2 days in amino-acid-containing medium supplemented with 2% horse serum (HS). (**b**) Effect of amino acids on myotube size. Cells were treated as described in **a**, except that the amino acid stimulation (+AA) was for 2 days. Histograms are means±s.e.m. for two assays. (**c**) Activity of the mTOR pathway in skeletal muscles of mice during starvation and refeeding. Shown is an immunoblot analysis of protein extracts from GC muscles of the indicated genotype, using anti-phospho-S6K1 Thr389, anti-4EBP1, anti-phospho-4EBP1 Ser65 and anti-rpL7a antibodies, the last as a loading control. Mice were starved for 48 h (St) and re-fed for 48 h (Rf). Control mice were fed randomly. (**d**) Weights of mouse body, fat and skeletal muscles after starvation and refeeding. Mice were treated as described in **c**, and the weights of epididymal fat pad, GC and TA muscles were evaluated. Data are means±s.e.m. for at least four mice per condition. *, $P<0.05$ versus randomly fed mice; #, $P<0.05$ versus starved mice.

In contrast, *S6K1*$^{-/-}$ and *S6K1*$^{-/-}$;*S6K2*$^{-/-}$ cells were refractory to rapamycin effect on size. In conclusion, *S6K1* deletion mimics the effects of rapamycin on cell size (Fig. 2d) but not on proliferation (Fig. 2a, b; Supplementary Fig. S2a). Thus, different signal transduction elements are required for the control of cell cycle and cell size by mTOR. S6K1 is dispensable for proliferation but is essential for muscle cells to increase in size.

To study growth in cells withdrawn from the cell cycle, we differentiated myoblasts to multinucleated myotubes by mitogen removal.

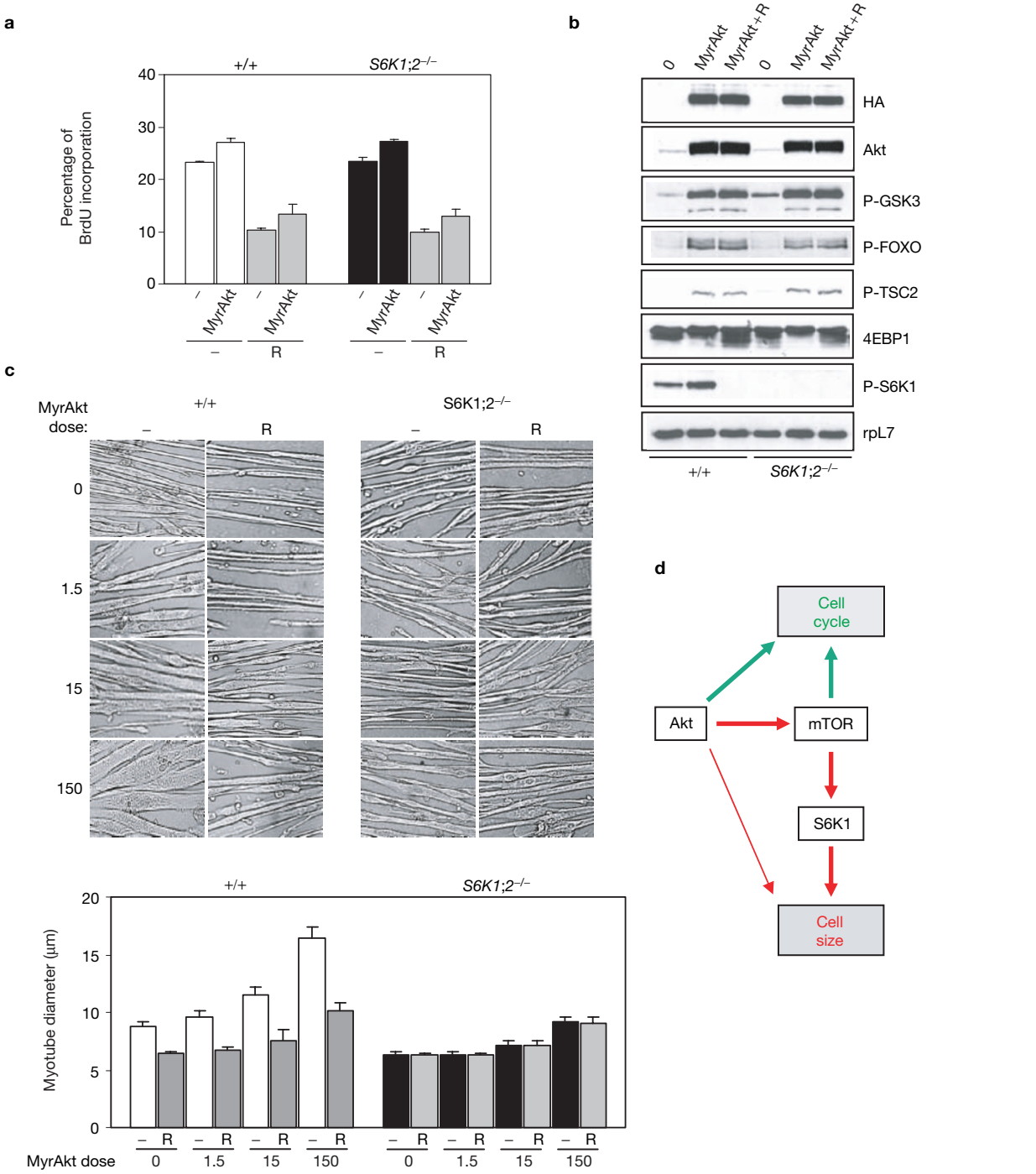

Figure 5 Regulation of muscle growth and proliferation by oncogenic Akt. (**a**) MyrAkt1 stimulates S-phase entry of both wild-type and *S6K1*$^{-/-}$;*S6K2*$^{-/-}$ cells. Myoblasts were transduced with MyrAkt1 (150 MOI), grown for 2 days in the presence or absence of 20 nM rapamycin (R) and incubated for 1 h with BrdU. Cells were stained with anti-BrdU antibodies and Hoechst 33258 to reveal S-phase and total nuclei, respectively. (**b**) MyrAkt1 signal transduction in myotubes. Immunoblot analysis of protein extracts from wild-type and *S6K1*$^{-/-}$/*S6K2*$^{-/-}$ myotubes with anti-HA (to reveal HA-tagged MyrAkt1), anti-phospho-TSC2 Ser 1462, anti-4E-BP1 (to reveal protein phosphorylation by electromobility shift), anti-phospho-S6K1 Thr 389, anti-phospho GSK3α/β Ser 21/9, anti-phospho-FKHR Thr 24 and anti-rpL7a antibodies, the last as a loading control. Cells were transduced with MyrAkt1 (150 MOI) at the myotube stage and harvested 2 days later for protein extraction. (**c**) S6K activity accounts for the rapamycin-sensitive hypertrophic response of myotubes to MyrAkt1. Bright-field images of wild-type and *S6K1*$^{-/-}$;*S6K2*$^{-/-}$ myotube cell cultures are shown. Myotubes were transduced with MyrAkt1 adenovirus at the indicated MOI. After 3 days in culture in 2% horse serum, myotube diameter was measured. The histograms are means ± s.e.m. for three experiments on one independent culture. At least 400 myotubes were analysed. (**d**) Schematic representation of mTOR-dependent and mTOR-independent branches regulating cell cycle and cell size in skeletal muscle cells. Pathways regulating cell cycle are represented in green, those regulating cell size in red. The thickness of the lines indicates the relative contribution of each pathway.

Four days later, both *S6K1*$^{-/-}$;*S6K2*$^{-/-}$ and wild-type cells were fully differentiated, as assessed by morphology and immunoblot of appropriate markers (Fig. 3a; data not shown). However, the diameter of *S6K1*$^{-/-}$;*S6K2*$^{-/-}$ myotubes was 22% smaller than that of the wild type (Fig. 3a). Examination of single mutants demonstrated that the small size phenotype was correlated with *S6K1* deletion (Fig. 3a). The number of nuclei per myotube was similar in wild-type and *S6K1*$^{-/-}$;*S6K2*$^{-/-}$ cells, confirming that *S6K1*$^{-/-}$;*S6K2*$^{-/-}$ muscle fibre atrophy is due to impaired cytoplasmic growth rather than to defective cell fusion (Supplementary Fig. S2b). Rapamycin blocks muscle differentiation by suppressing IGF2 production[4]. IGF2 or IGF1 rescues cell differentiation but not myotube size in the presence of rapamycin, indicating that mTOR initiates differentiation and growth through independent mechanisms[4]. In agreement with this, we identify S6K1 as a critical growth-promoting element that does not affect myogenesis.

To analyse the regulation of growth by IGFs, we asked whether S6K deletion was sufficient to impair the hypertrophic response of myotubes to IGF1. Two days after differentiation, cells were treated with IGF1 for 2 days. This did not change the number of myonuclei in wild-type or *S6K1*$^{-/-}$;*S6K2*$^{-/-}$ myotubes (Supplementary Fig. S2b), indicating that the processes of differentiation and fusion were completed when IGF1 was added. IGF1 induced a 35–50% increase in wild-type myotube diameter (Fig. 3a). Consistent with earlier observations[1], rapamycin blocked this response by about 70%, suggesting that the mTOR pathway contributes in part to IGF1-promoted hypertrophy. As expected, IGF1 stimulated and rapamycin inhibited S6K and 4EBP1 phosphorylation (Fig. 3b). IGF1-induced cell growth and rapamycin inhibition was significantly blunted in *S6K1*$^{-/-}$;*S6K2*$^{-/-}$ cells (Fig. 3a), a phenotype that was correlated with *S6K1* deletion (Fig. 3a). Moreover, *S6K1*$^{-/-}$ and *S6K2*$^{-/-}$ cells showed rpS6 phosphorylation levels comparable to those in wild-type cells, and both gene deletions were required to affect rpS6 phosphorylation (Fig. 3b). Thus, myotubes lacking S6K1 have an impaired hypertrophic response to IGF1, which is not correlated with rpS6 phosphorylation levels.

Next we overexpressed S6K1 and S6K2 in myotubes. Both kinases rescued rpS6 phosphorylation in *S6K1*$^{-/-}$;*S6K2*$^{-/-}$ cells (Fig. 2c). Expression of S6K1, but not S6K2, was sufficient to increase cell size in wild-type and *S6K1*$^{-/-}$;*S6K2*$^{-/-}$ myotubes. This effect was mimicked by RR-S6K1, which also conferred partial protection against rapamycin (Fig. 3c). Thus, S6K1 and S6K2 are functionally redundant with regard to rpS6 phosphorylation, but S6K2 cannot compensate for the growth defect due to S6K1 deletion. These data indicate that one or more unidentified S6K1 substrates could promote cell growth.

To investigate whether other known mTOR substrates, besides S6K1, signal to increased muscle growth, we analysed the effect of distinct *4EBP1* alleles on myotube size. Cells expressing 4EBP1-WT and 4EBP1-A presented myotube sizes comparable to that in the control, and expression of the 4EBP1 partner, eIF4E, also failed to modify the size of both wild-type and *S6K1*$^{-/-}$;*S6K2*$^{-/-}$ myotubes (Supplementary Fig. S3). Evidence that 4EBPs do not have a major function in skeletal muscle growth also came from gene targeting in mice, because the GC muscle mass of mice lacking *4EBP1* and *4EBP2* genes was equivalent to that of the wild type (Olivier Le Bacquer and N.S., unpublished data). Taken together, our findings point towards a specific function of S6K1 in skeletal muscle growth that is not shared by other known mTOR substrates such as S6K2, 4EBP1 and 4EBP2.

S6K is distinct because it requires activation signals from both growth factors and amino acids[9], which confer on the enzyme the potential of coordinating growth depending on the nutritional state. Amino-acid starvation of wild-type cells attenuated S6K1 activity, followed by upregulation after the re-addition of nutrients (Fig. 4a). Whereas wild-type cells shrank after starvation and recovered their size after re-exposure to amino acids, *S6K1*$^{-/-}$;*S6K2*$^{-/-}$ myotubes failed to adapt their size as a function of amino acid availability (Fig. 4b). This prompted us to analyse muscle mass in the animal after 2-day starvation and 2-day refeeding periods, which influenced S6K activity and 4EBP1 phosphorylation as predicted (Fig. 4c). Mice from both genotypes lost about 25% of their weight after starvation, and almost completely recovered their initial body weight after refeeding (Fig. 4d). However, analysis of muscle mass in comparison with fat mass revealed tissue-specific differences. After starvation, loss of adipose tissue from the epididymal fat pad was more pronounced in the S6K-deficient mice. In contrast, starvation decreased the mass of wild-type TA and GC muscles by about 35%, without affecting muscle weight of *S6K1*$^{-/-}$;*S6K2*$^{-/-}$ mice (Fig. 4d), even though 4EBP1 was dephosphorylated in these conditions (Fig. 4c). Refeeding of wild-type mice led to partial recovery of muscle mass with no changes in fat weight, whereas in *S6K1*$^{-/-}$;*S6K2*$^{-/-}$ mice the opposite tendency was observed (Fig. 4d). Thus, in S6K-deficient mice, nutrient availability fails to modify muscle mass.

The constitutively active form of Akt (MyrAkt1) is a master regulator of muscle growth[1,2,5,6]. This oncogenic kinase exerts a longlasting regulation on multiple substrates such as GSK3, the FOXO proteins, BAD and TSC2 (refs 9, 20). TSC2 is required for the control of mTOR activity by growth factors and nutrients[9]. Overexpression of MyrAkt1 significantly increased the rate of S-phase entry in wild-type myoblast cells (Fig. 5a). The effect of MyrAkt1 could also be detected in rapamycin-treated cells or in *S6K1*$^{-/-}$;*S6K2*$^{-/-}$ cells, indicating that the myoblast cell cycle is controlled by Akt and mTOR through two separate pathways, both of which are independent of S6K.

To evaluate the effect of MyrAkt1 on cell size, we transduced MyrAkt1 into myotubes. In wild-type cells this resulted in the phosphorylation of Akt substrates: GSK3, FOXO1 and TSC2 (Fig. 5b). Consistent with a regulatory function of TSC2 phosphorylation on the activity of the mTOR pathway[9], the phosphorylation of S6K1 and 4EBP1 was also induced by MyrAkt1 expression in a rapamycin-sensitive manner (Fig. 5b). In wild-type cells, MyrAkt1 transduction led to a dose-dependent increase in myotube diameter. Rapamycin treatment strongly, but not completely, inhibited MyrAkt1 action, indicating that both mTOR-dependent and mTOR-independent branches of Akt signalling mediate hypertrophy (Fig. 5c). Conversely, in *S6K1*$^{-/-}$;*S6K2*$^{-/-}$ cells, low levels of MyrAkt1 expression failed to increase size, whereas the highest dose of MyrAkt1 induced hypertrophy. This response was insensitive to rapamycin, whereas 4EBP1 phosphorylation was efficiently blocked by the drug (Fig. 5b). *S6K1*$^{-/-}$ cells displayed the same defective response to MyrAkt1 as the double mutant (Supplementary Fig. S4). In conclusion, we demonstrate three main points represented in Fig. 5d. First, the effectors of Akt and mTOR regulating muscle cell cycle are distinct and do not include S6K. Second, S6K1 is required for mTOR-mediated growth triggered by oncogenic Akt1, indicating that other mTOR effectors are not involved in this response or that their action depends on S6K1 activity. Last, a pathway independent of mTOR cooperates with S6K1 to control Akt-induced growth. The inactivation of GSK3 and FOXO1 by phosphorylation could

fulfil such a function[1,5,6]. The relative contribution of this rapamycin-insensitive pathway increases as a function of MyrAkt activity, although it remains lower than the contribution by S6K1.

The TOR pathway controls both cell cycle progression and cell growth, a function maintained through evolution from yeast to mammals. In yeast the effect of TOR on cell cycle is secondary to the regulation of cell growth, because yeast must reach a certain size to divide[21]. Here we show that the growth and proliferation of muscle cells require distinct effectors of mTOR, which is consistent with the idea that in mammals separate mechanisms evolved in the regulation of these processes[22,23]. In particular, we show that growth, but not proliferation, requires S6K1. In a broader view, these findings could be relevant for improving current therapies. It can be envisaged that S6K1 activation would lead to a recovery of muscle mass with a low risk of neoplasm in cases of muscle atrophy as a consequence of AIDS, ageing, and bed rest after surgery. In addition, mTOR inhibition by rapamycin analogues is being used for immunosuppression after organ transplantation, and in clinical trials for cancer therapy. Targeting distinct mTOR effectors might represent a more efficacious therapeutic strategy, given the high degree of downstream signalling specificity. □

METHODS

Animals. Targeted disruption of *S6K1* and *S6K2* loci, and confirmation of the lack of protein in homozygous mutant mice, have been described previously[17,24]. Animals were initially in the mixed C57Bl/6-129Ola genetic background and then backcrossed ten times to a 'pure' C57Bl/6 background. The data shown in this study were first obtained in mice of a mixed genetic background and then confirmed in C57Bl/6 mice. No phenotypic differences in muscle growth were observed as a function of the genetic background. Because the combined mutation of S6K1 and S6K2 was lethal in the C57Bl/6 background, adult mice of this genotype had a mixed background and were compared with the proper wild-type control. Animals were maintained on a 12 h:12 h light/dark cycle and were allowed free access to food. Mice were genotyped by polymerase chain reaction analysis of tail DNA with the following primers: S6K1 sense, 5′-GTAGGGCACTTAAATGACCAC-3′; S6K1 antisense, 5′-TGTCCCTATTAATGCTCAAGG-3′; S6K2 sense, 5′-ACTGTTGACCCAACTCTGAAAG-3′; S6K2 antisense, 5′-CGTCTGCCGTGTGAATCGTG-3′; neomycin resistance gene antisense, 5′-GCCTTCTTGACGAGTTCTTCTGAG-3′. For starvation/refeeding experiments, mice were deprived of food for 2 days and then allowed free access to food for a further 2 days. All experimental designs and procedures were performed in accordance with the guidelines of the animal ethics committee of the Ministère de l'Agriculture of France.

Histology. Soleus and TA muscles of 5-week-old male mice were embedded in 7% gum tragacanth (Acros Organics), frozen in isopentane chilled in liquid nitrogen and stored at −80 °C. Transverse cross-sections 5 µm thick were collected along the entire length of the muscle at 400 µm intervals with a cryostat (Leica CM 1850) and stained with haematoxylin/eosin solution. The sections with the largest CSA were used for analysis. To quantify muscle size, fibre size and fibre number, sections were analysed on a Nikon E800 microscope equipped with a video camera and Lucia archive software. To determine fibre type, sections were immunostained with anti-type I and anti-type II myosin heavy chain (MyHC) monoclonal antibodies (Sigma) at 1:5,000 and 1:500 dilution, respectively. The primary antibody was detected with Vectastain Elite ABC reagent (Vector) and 3,3′-diaminobenzidine tetrahydrochloride-plus coloration kit (Zymed), in accordance with the instructions of the manufacturers. All fibres expressing type I (slow) or type II (fast) MyHC were counted in one section. To evaluate the number of nuclei per fibre, sections were incubated with anti-dystrophin monoclonal antibody (Novocastra; 1:50 dilution) at room temperature for 3 h. After being washed in phosphate-buffered saline (PBS), sections were incubated with fluorescein isothiocyanate-conjugated goat anti-mouse IgG1 (Southern Biotechnology Associates; 2 µg ml^{-1}). After further washing, sections were stained with Hoechst 33258 (ACROS; 200 ng ml^{-1}) and mounted. Nuclei within the dystrophin-positive sarcolemma were counted in each myofibre of the entire muscle section.

Plasmids and viral vectors. The following adenovirus vectors were used: haemagglutinin (HA)-tagged MyrAkt1, HA-tagged kinase inactive Akt1 in which Thr 308 and Ser 473 had been mutated to Ala residues, Myc-tagged wild-type p70S6K1 and S6K2, and Myc-tagged rapamycin resistant p70 S6K1 in which Thr 389 and Thr 421 had been mutated to Glu residues and Ser 411, Ser 418 and Ser 424 had been mutated to Asp residues. For transient transfection, the HA-tagged versions of eIF4E, wild-type 4EBP1 and 4EBP1-A (Thr 37, Thr 46, Ser65 and Thr 70 mutated to Ala) were subcloned into pcDNA3. For retroviral production, 4EBP1-WT or 4EBP1-A was subcloned into the MSCV-IRES–GFP plasmid.

Cell cultures. Primary cultures were derived from GC and TA muscles of 4-week-old mice, as described[25]. In brief, muscles were partly digested with four sequential 10-min incubations in DMEM/HamF12 medium containing 0.14% pronase (Gibco). The supernatants from the second, third and fourth digestions were pooled and filtered through a 100-µm cell strainer. Cells were centrifuged, washed twice, counted and plated at low density (100 cells cm^{-2}) on 12-well plates coated with gelatin (Type A from pig skin; Sigma). Cells were grown in complete medium composed of DMEM/Ham F12 (Gibco), 2% Ultroser G (Biosepra), 20% fetal calf serum (Gibco), penicillin, streptomycin and L-glutamine. After 1 week, wells containing myoblasts without contaminating fibroblasts were trypsinized, pooled and expanded. Experiments were performed on cells kept in culture for not more than 1 month (6–15 passages). Complete medium was changed every 2 days, and cultures were trypsinized before subconfluence to avoid differentiation.

To assay cell-doubling time, cells were seeded on gelatin-coated six-well plates at a density of 270 cells cm^{-2}, grown in complete medium and trypsinized. Viable cells were counted every day on a haemocytometer with Trypan blue dye. Each time point was measured in triplicate.

For BrdU labelling, cells were seeded at a density of 250 cells cm^{-2} on two-well LabTek plates coated with Matrigel (Becton Dickinson) and kept in complete medium. When indicated, 1 day after seeding, cells were transduced with adenovirus vectors for 1 h in DMEM/HamF12 medium containing 2% horse serum, washed and then switched back to complete medium. Three days after seeding, cells were incubated for 1 h with BrdU (6 µg ml^{-1}), washed and fixed in 4% paraformaldehyde at room temperature for 15 min. Samples were boiled for 10 min in citrate buffer and immunostained with monoclonal anti-BrdU antibody (Roche) and Texas red-conjugated secondary antibodies (Jackson Laboratories). Cells were stained with Hoechst 33258 and mounted. The percentage incorporation of BrdU was determined by counting the BrdU-positive nuclei among at least 1,000 nuclei in distinct fields.

For analysis by fluorescence-activated cell sorting, cells were plated in gelatin-coated 10-cm dishes at a density of 900 cells cm^{-2}. Three days later, cells were washed with PBS and incubated at 37 °C for 8 min in 4 ml of PBS/EDTA (2.5 mM). Cells were collected and centrifuged at 1,000*g* for 5 min in a conical tube. Cell pellets were thoroughly resuspended in 0.5 ml of PBS, fixed by slowly adding 70% ethanol and stored at −20 °C. For DNA content analysis, fixed cells were centrifuged, washed with PBS and resuspended in 1 ml of 1% fetal calf serum in PBS containing 100 µg ml^{-1} RNase A. After incubation at 37 °C for 30 min, propidium iodide at a final concentration of 20 µg ml^{-1} was added to the solution immediately before analysis on a BD-LSR flow cytometer (Becton Dickinson) equipped with an argon laser (emission wavelength 488 nm) and CellQuest software. Fluorescence data were obtained from 20,000 viable cells and detected in the FL-2 channel to distinguish cells with a DNA content of 2*N* and 4*N*. Doublet cells were gated away by using the ratio between FL-2 area and FL-2 width. To assess cell size, the intensity of forward scatter height was measured by selecting the logarithmic mode of the amplifier, previously calibrated with Calibrite microsphere standards (Molecular Probes).

To differentiate muscle cells, myoblasts were plated on Matrigel-coated dishes at 20,000 cells cm^{-2}. After 6 h, cells were switched to DMEM/Ham F12 containing 2% horse serum. To measure the hypertrophic response of IGF1, myotubes at day 2 of differentiation were incubated with 250 ng ml^{-1} IGF1-R3 (Sigma) for a further 2 days in DMEM/Ham F12 containing 0.2% BSA (Albumax; Gibco). The effect of amino acids on size was evaluated by starving the myotubes at day 3 of differentiation in amino-acid-free DMEM containing 0.2% BSA, and stimulating for a further 2 days in DMEM/Ham F12 containing 0.2% BSA. To measure the effect of MyrAkt1 and S6K, myotubes at day 2 of differentiation were transduced with adenovirus as described above, washed and incubated for a further 2–3 days in DMEM/Ham F12 containing 2% horse serum. Bright-field images of live cells

were randomly taken and analysed by the Lucia archive software. The diameters of at least 400 myotubes were measured in a region where myonuclei were absent and diameter was constant. To count the number of nuclei per cell, myotubes were fixed in 2% paraformaldehyde and stained with Hoechst 33258. The number of nuclei in at least 500 myotubes was counted with the Lucia archive software.

Retrovirus-mediated production of stable cell lines. To produce retroviruses, the MSCV-IRES–GFP plasmids expressing 4EBP1 were transfected in Ecotropic 293T Phoenix cells with the use of Lipofectamine Plus reagent (Invitrogen). The medium was collected, passed through a 0.45-μm filter and frozen as aliquots 48 h after transfection. To generate stable cell lines co-expressing 4EBP1 constructs and GFP, myoblasts were seeded in 60-mm dishes and infected by adding one volume of retroviral supernatant and one volume of 30% FBS, 4% Ultroser G and 5 μg ml^{-1} Polybrene. Transduction was repeated daily three times and the retroviral supernatant was then replaced with complete medium. GFP-positive myoblasts were selected and collected by cell sorting with FACSvantage SE. After collection, cells were grown for two to three passages and used for experiments.

Transient transfections. Myoblasts were seeded in 6-cm dishes and myotubes were transfected after 2 days of differentiation. For each dish, 3 μg of plasmid expressing GFP and 12 μg of pRK5 empty vector (control) or plasmid expressing HA-S6K1, HA-eIF4E, HA-4EBP1-WT or HA-4EBP1-A were complexed with 12 μl of Lipofectamine 2000 (Invitrogen) in 1 ml of Opti-MEM medium (Life Technologies) for 20 min at room temperature. The Lipofectamine–DNA complex was added to the myotubes and incubated for 4 h at 37 °C in the presence of 3 ml of differentiation medium without antibiotics. The transfection medium was then replaced with fresh differentiation medium. At 48 h after transfection, pictures of the cells were taken under phase contrast and a fluorescent filter, and the sizes of GFP-positive and GFP-negative myotubes were analysed.

Immunoblotting. Cells were washed twice with cold PBS, scraped off of the culture dish in lysis buffer B (50 mM Tris-HCl pH 8, 1% Nonidet P40, 120 mM NaCl, 20 mM NaF, 1 mM benzamidine, 1 mM EDTA, 1 mM EGTA, 15 mM sodium pyrophosphate, 1 mM phenylmethylsulphonyl fluoride, 2 mM sodium orthovanadate, 2 μg ml^{-1} leupeptin, 5 μg ml^{-1} aprotinin, 1 μg ml^{-1} pepstatin A) and sonicated for 30 s. To remove cell debris, homogenates were centrifuged at 8,000*g* for 10 min at 4 °C. Protein extract was resolved by SDS–PAGE before transfer to a nitrocellulose membrane and incubation with the following primary antibodies: rabbit anti-S6K1 (provided by G. Thomas), anti-rpL7a (provided by A. Ziemiecki), anti-GFP (provided by R.E. Jensen), anti-myogenin (Santa Cruz Biochemicals), anti-phospho-Ser 240/244 and 235/236 rpS6, anti-phospho-Thr 389 S6K1, anti-4EBP1, anti-phospho-GSK3α/β Ser 21/9, anti-phospho-TSC2 Ser 1462, anti-phospho 4EBP1 Ser 65, anti-FKHR Thr 24 (Cell Signaling Technologies), and monoclonal anti-MyHC (MF20; Sigma), anti-actin (Sigma) and anti-HA (Roche).

Note: Supplementary Information is available on the Nature Cell Biology website.

ACKNOWLEDGEMENTS
We thank the Novartis Foundation and George Thomas laboratory for the use of S6K mutant mice. We thank J. McMullen, G. Pavlath, R. Scharfmann, G. Thomas and R. Treisman for reading the manuscript and for helpful discussions; the members of INSERM-U584 for support; Genethon (Evry) for adenovirus production; C. Cordier for expert technical assistance with the FACS analysis; M. Birnbaum for providing adenovirus expressing MyrAkt1 and kinase-inactive Akt1; and G. Thomas for providing adenovirus expressing RR-S6K1. M.P. has been a recipient of a stipend from the Fondation pour la recherche médicale, and A.S. from the INSERM and Conseil Regional d'Ile de France. This work was supported by a grant to M.P. from the INSERM Avenir programme (R01131KS) and from INSERM-Fondation pour la recherche médicale–Juvenile Diabetes Research Foundation International (4DA03H), and to A.S. and M.P. from the Association Française contre les Myopathies (9971) and from the ARC (7647).

COMPETING FINANCIAL INTERESTS
The authors declare that they have no competing financial interests.

Received 6 December 2004; accepted 17 January 2005
Published online at http://www.nature.com/naturecellbiology

1. Rommel, C. *et al.* Mediation of IGF-1-induced skeletal myotube hypertrophy by PI(3)K/Akt/mTOR and PI(3)K/Akt/GSK3 pathways. *Nature Cell Biol.* **3,** 1009–1013 (2001).
2. Bodine, S.C. *et al.* Akt/mTOR pathway is a crucial regulator of skeletal muscle hypertrophy and can prevent muscle atrophy *in vivo*. *Nature Cell Biol.* **3,** 1014–1019 (2001).
3. Pallafacchina, G., Calabria, E., Serrano, A.L., Kalhovde, J.M. & Schiaffino, S. A protein kinase B-dependent and rapamycin-sensitive pathway controls skeletal muscle growth but not fiber type specification. *Proc. Natl. Acad. Sci. USA* **99,** 9213–9218 (2002).
4. Erbay, E., Park, I.H., Nuzzi, P.D., Schoenherr, C.J. & Chen, J. IGF-II transcription in skeletal myogenesis is controlled by mTOR and nutrients. *J. Cell Biol.* **163,** 931–936 (2003).
5. Sandri, M. *et al.* Foxo transcription factors induce the atrophy-related ubiquitin ligase atrogin-1 and cause skeletal muscle atrophy. *Cell* **117,** 399–412 (2004).
6. Stitt, T.N. *et al.* The IGF-1/PI3K/Akt pathway prevents expression of muscle atrophy-induced ubiquitin ligases by inhibiting FOXO transcription factors. *Mol. Cell* **14,** 395–403 (2004).
7. Glass, D.J. Molecular mechanisms modulating muscle mass. *Trends Mol. Med.* **9,** 344–350 (2003).
8. Abraham, R.T. Identification of TOR signaling complexes: more TORC for the cell growth engine. *Cell* **111,** 9–12 (2002).
9. Manning, B.D. & Cantley, L.C. Rheb fills a GAP between TSC and TOR. *Trends Biochem. Sci.* **28,** 573–576 (2003).
10. Coolican, S.A., Samuel, D.S., Ewton, D.Z., McWade, F.J. & Florini, J.R. The mitogenic and myogenic actions of insulin-like growth factors utilize distinct signaling pathways. *J. Biol. Chem.* **272,** 6653–6662 (1997).
11. Huang, S. *et al.* Sustained activation of the JNK cascade and rapamycin-induced apoptosis are suppressed by p53/p21(Cip1). *Mol. Cell* **11,** 1491–1501 (2003).
12. Montagne, J. *et al.* Drosophila S6 kinase: a regulator of cell size. *Science* **285,** 2126–2129 (1999).
13. Zhang, H., Stallock, J.P., Ng, J.C., Reinhard, C. & Neufeld, T.P. Regulation of cellular growth by the *Drosophila* target of rapamycin dTOR. *Genes Dev.* **14,** 2712–2724 (2000).
14. Miron, M. *et al.* The translational inhibitor 4E-BP is an effector of PI(3)K/Akt signalling and cell growth in *Drosophila*. *Nature Cell Biol.* **3,** 596–601 (2001).
15. Fingar, D.C., Salama, S., Tsou, C., Harlow, E. & Blenis, J. Mammalian cell size is controlled by mTOR and its downstream targets S6K1 and 4EBP1/eIF4E. *Genes Dev.* **16,** 1472–1487 (2002).
16. Fingar, D.C. *et al.* mTOR controls cell cycle progression through its cell growth effectors S6K1 and 4E-BP1/eukaryotic translation initiation factor 4E. *Mol. Cell. Biol.* **24,** 200–216 (2004).
17. Pende, M. *et al.* S6K1$^{(-/-)}$/S6K2$^{(-/-)}$ Mice exhibit perinatal lethality and rapamycin-sensitive 5′-terminal oligopyrimidine mRNA translation and reveal a mitogen-activated protein kinase-dependent S6 kinase pathway. *Mol. Cell. Biol.* **24,** 3112–3124 (2004).
18. Pende, M. *et al.* Hypoinsulinaemia, glucose intolerance and diminished beta-cell size in S6K1-deficient mice. *Nature* **408,** 994–997 (2000).
19. Gingras, A.C. *et al.* Hierarchical phosphorylation of the translation inhibitor 4E-BP1. *Genes Dev.* **15,** 2852–2864 (2001).
20. Whiteman, E.L., Cho, H. & Birnbaum, M.J. Role of Akt/protein kinase B in metabolism. *Trends Endocrinol. Metab* **13,** 444–451 (2002).
21. Lorberg, A. & Hall, M.N. TOR: the first 10 years. *Curr. Top. Microbiol. Immunol.* **279,** 1–18 (2004).
22. Conlon, I. & Raff, M. Differences in the way a mammalian cell and yeast cells coordinate cell growth and cell-cycle progression. *J. Biol.* **2,** 7 (2003).
23. Dolznig, H., Grebien, F., Sauer, T., Beug, H. & Mullner, E.W. Evidence for a size-sensing mechanism in animal cells. *Nature Cell Biol.* **6,** 899–905 (2004).
24. Shima, H. *et al.* Disruption of the p70(s6k)/p85(s6k) gene reveals a small mouse phenotype and a new functional S6 kinase. *EMBO J.* **17,** 6649–6659 (1998).
25. Pinset, C. & Montarras, D. in *Cell Biology, a Laboratory Handbook* (ed. Celis, J.) 226–232 (Academic, New York, 1998).